Simultaneous Reduction of Oxides and Dissolution of Alumina in Stainless Steelmaking Slag

M. Divakar, M. Görnerup[*1] and A. K. Lahiri

[*]Uddeholm Technology AB, Uvåv. 2, S-68340, Uddeholm, Sweden.
Department of Metallurgy, Indian Institute of Science, Bangalore - 560 012, India

ABSTRACT

During stainless steelmaking a number of phenomena like slag formation, reduction of oxides and foam formation take place simultaneously. Independently each of these phenomena has been studied by a number of investigators. However little information is available on the simultaneous occurrence of different phenomena. Experiments have been conducted to study the simultaneous reduction of oxides of chromium, vanadium and iron from stainless steelmaking slag by carbon along with the dissolution of alumina in the slag. Results show that the interaction is complex.

1. Introduction

The reduction of oxides by carbon in stainless steelmaking slags is a complex phenomenon due to simultaneous gas generation, foam formation and stirring of the slag melt. The reduction reactions can be represented in the following way

$$MO_x + (y+x)C[solid/solute] = MC_y + xCO$$
$$MO_x + xCO(g) = M + xCO_2(g)$$

The formed CO_2 gas can further react with carbon forming CO according to the Boudouard reaction. Due to the complexity of the system, the rate limiting step in the reduction of oxides differs as the conditions for the reaction are changed. Both mixed control[1,2] and diffusion control[3,4] have been reported as rate limiting steps for the reduction of Cr_2O_3. The rate

[1] At the time of work the author was at the Department of Metallurgy, KTH, S-10044, Stockholm, Sweden.

limiting step for FeO reduction has been reported to vary with its amount in the slag. In high FeO content systems, diffusion[5], chemical reaction[6,7] or mixed control[8] are stated to be rate limiting. At lower FeO levels (<10%) mass transport of FeO was found[7] to be the rate limiting step.

In the present study, the focus is on the phenomena that take place during simultaneous reduction of oxides by carbon and their influence on the reduction kinetics of Cr_2O_3 under typical electric stainless steelmaking conditions.

2. Experimental Technique

2.1. Experimental Equipment

The furnace was heated by resistance heating elements of $MoSi_2$ (Kanthal-type). The furnace was controlled manually and had a maximum operating temperature of 1650°C. The temperature was monitored by a B-type thermocouple (Pt-6%Rh/Pt-30%Rh) placed in direct contact with the graphite crucible bottom. The furnace had a constant temperature zone (±5°C) over a length of 80mm and the maximum temperature deviation from given experimental value over a shorter period of time was ±12°C.

The graphite crucible was held in the 900mm long sintered alumina furnace tube. The tube had an inner diameter of 64mm. The furnace tube was continuously flushed by argon and the alumina tube was sealed gas tight in the lower end. In the upper end, where charging and sampling took place, a ceramic lock was placed which was open during sampling. This ceramic lid was not gas tight but had a fairly good fit in order to give a reasonably good protection against air penetration. The furnace steel shell had a window of aluminum metal allowing the x-rays to penetrate the furnace tube at the crucible position. The x-rays covered a limited cross section and consequently the furnace had to be mobile in the vertical direction so that different levels in the crucible can be studied. The x-ray equipment consisted of a x-ray generator (70kV, 200mA), receiver, VHS Video camera with recorder and a monitor.

2.2. Experimental Procedure

The furnace was superheated to approximately 20°C above the experimental temperature and the graphite crucible containing 50gm of the premelted slag and lined with an alumina tube was slowly moved downwards into the furnace. This was done to avoid the furnace alumina tube from cracking. After approximately five minutes the experimental position was reached and within a few minutes the experimental temperature was reached. The x-ray equipment was used to establish the point of melting in order to set time to zero, defined as the time when all the slag has melted which can be clearly seen on the screen of the x-ray monitor.

Slag sampling was done after 3, 7, 12, 18, 28, 38 etc., minutes until the experiment was stopped. The foaming grade was studied by intermediate x-ray recording stored on videotape. Continuous exposure to the x-rays for more than two minutes was not possible owing to the risk of overheating the equipment, however, short 'beam bursts' of 0.5-1 minute every other minute was sufficient in order to follow the foaming. When the gas generation was considered low, the experiment was stopped by removing the crucible and quenching the slag in air.

Table I gives a typical slag composition used in the EAF stainless steelmaking which was chosen for this study. Starting from this composition the levels of all the components were changed. Every composition was investigated at 1550 and 1600°C and a few were studied at 1650°C also. In addition to these, two compositions with different levels of V_2O_5 were also studied at the three temperatures. Forty-three experiments have been conducted on slag samples in the temperature range of 1550-1650°C. The slag compositions are listed in Table II. In each of the experiments, the slag samples collected at different time intervals were analyzed. The respective amounts of oxides were determined assuming that weight of CaO in the slag remained unchanged.

All slag samples were analyzed in the sequenced differentiated x-ray spectrometer, Siemens SRS-303. The maximum relative error when using this equipment is ±2%. The slag foaming was measured manually on a monitor by watching a total of 20.5 hours of video recording.

3. Results

The video recording of the experiment was viewed to follow the reaction process. The x-ray recording was not very clear due to the limitations of the camera resolution, however, several phenomena could be observed from the video recording during the reduction process. These include steady, intermittent or vigorous gas generation, foam formation, variation in foam height and bubble size and stirring of the slag. Liquid metal droplets of various sizes were also seen both at the bottom of the crucible and in the foam during the progress of the reaction. During the gas generation, the bubble size varied with time. Figure 1 shows a x-ray image of the reduction process where gas generation at the bottom of the crucible, gas bubble coalescence and bubble burst at the top of the slag could be seen. It can also be seen that gas generation did not take place uniformly at the bottom of the crucible. Figure 2 shows another x-ray image of the reduction process where gas evolution was seen around iron droplets and bubble coalescence at the top. Figures 1 and 2 are typical x-ray pictures grabbed from the video recording during the reduction process and edited in a software package to improve the contrast.

During the reduction process, in some cases the gas bubbles moved independently inside the slag forming an emulsion. However, in most of the cases the gas bubbles were interconnected by slag films resulting in the formation of foam which moved upwards in the crucible. The height of foam was measured manually from the video recording at different time intervals. Figures 3 and 4 are typical plots showing the rate of gas evolution and change in foam height during the reaction. Figure 3 shows that the gas generation rate reaches a maximum of about 0.24 lt./min within 10 minutes and then decreases monotonically. On the other hand, the foam height remains less than 10mm until 30 minutes and then rises to a maximum of 28mm at about 60 minutes when the gas generation rate was quite low. In Fig. 4 the foam height reaches a maximum of about 36mm within 5 minutes of the reaction, remains at the maximum height up to 30 minutes and falls continuously. The gas generation rate shows two maxima, first maximum of about 0.24 lt./min within 3 minutes of the reaction and the second of about 0.31 lt./min at about 50 minutes. Normally the foam height increases with the gas generation rate[9] as is seen in Fig. 4 during the first few minutes. On the other hand, Fig. 3 and later portion of Fig. 4 show that the foam height is not proportional to the gas generation rate. Similar behavior was observed in other slags also. Hence, it can be inferred that there was no direct relationship between the gas generation rate and the foam height.

Figure 5 shows the variation of weights of the oxides with time in one of the slag compositions studied at 1823 K. The graph shows a steep rise in the Al_2O_3 content of the slag melt followed by a saturation stage. CaO and SiO_2 remain unchanged in their respective weights throughout the reaction period. The inset in the figure shows the variation of other oxides that are grouped in the lower portion of the figure. MnO is not reduced while FeO, Cr_2O_3 and V_2O_5 are reduced. It can be noticed from the data that the slag composition was changing continuously during the experiment owing to the dissolution of Al_2O_3 to a large extent and the reduction of several oxides. It was found in certain slags that the dissolution of Al_2O_3 reached the saturation level of the ternary $CaO\text{-}SiO_2\text{-}Al_2O_3$ system at respective temperatures. In some slags the Al_2O_3 content increased from the initial level of 7% to about 53% where the total weight of the slag increased from 50gm to 88gm. Hence the total weight of the slag varied significantly with time.

As a first approximation, reaction rate for Cr_2O_3 reduction can be represented as,

$$-\frac{dW_{Cr_2O_3}}{dt} = \alpha\left(\%Cr_2O_3 - \%Cr_2O_3^{eq}\right) \qquad (1)$$

where 'α' is the apparent rate constant, $\%Cr_2O_3$ is the amount present at any time 't' and $\%Cr_2O_3^{eq}$ is the amount present in the slag in equilibrium with graphite. Equation (1) is usually written in the following manner,

$$-\frac{W_o d\%Cr_2O_3}{dt} = \alpha\left(\%Cr_2O_3 - \%Cr_2O_3^{eq}\right) \qquad (2)$$

where W_o is the total weight of the slag. Since the total weight of the slag was changing in the present case, Eqn. (2) could not be used for integration. The term $\%Cr_2O_3^{eq}$ is very low, 20--50 ppm[10], and is neglected. Integrating Eqn. (1) from t = 0 to t = t we have,

$$W^o{}_{Cr_2O_3} - W_{Cr_2O_3} = \alpha\int_o^t \%Cr_2O_3 dt \qquad (3)$$

where W^{o}_{Cr2O3} and W_{Cr2O3} are the initial weight and weight at any time 't' of Cr_2O_3 respectively. The right hand side of Eqn. (3) was evaluated numerically using the trapezoidal rule. The apparent rate constant can be determined by plotting the left-hand side term against the numerically evaluated integral. Figure 6 shows a typical plot of the reaction process. In general, the plots show two regions of the reaction, the varying rate at the beginning followed by a steady state region. It was established[11] that Cr_2O_3 reduction takes place primarily at the metal droplet/slag interface where the iron droplets saturated with carbon act as sites for the reduction. The varying rate period refers to the formation of liquid iron droplets. All the curves were almost straight lines in the steady state region and the apparent rate constant was obtained by means of linear regression in this region. This procedure is carried out at all the temperatures for a given slag composition. It was interesting to note that though there was a sharp dissolution of Al_2O_3 into the slag in the steady state region, the rate of Cr_2O_3 reduction was not affected in the slags.

3.1. Effect of Cr_2O_3 Content

During the reduction experiments, the foam height and gas generation rate varied with time but they had no relationship. The maximum foam height and foam stability increased with increasing Cr_2O_3 content in the slag. Swisher and McCabe[12] showed that Cr_2O_3 increased the foam life of CaO-SiO_2 slags within the completely liquid region of the slag composition. The present observation is in conformity with their work. Figure 7 shows the variation of rate constant (α) with initial wt% Cr_2O_3 in the slags at 1823 K. It can be noticed that the rate constant decreases with increasing Cr_2O_3 content of the slag. Figure 8 shows the variation of wt% Cr_2O_3/wt% FeO ratio with time for different slags containing 6% FeO at 1823 K. It is clear from this figure that the ratio increased continuously almost throughout the reduction period. This indicates that FeO is reduced faster than Cr_2O_3.

3.2. Effect of MgO Content

The effect of MgO content in the slag on the observed phenomena is complex. In slags containing 0 and 5% MgO the foam height was significant (28mm-36mm) and the foam was stable for long periods (20-25 minutes). At higher contents of MgO (10 and 15%) the foam height was quite low (5-10mm) but was stable for longer periods of time (40-50 minutes).

Ito and Fruehan[9] found that addition of MgO to CaO-SiO_2-FeO slags increased the foaming index, which is also related to the foam stability. In the present study we observed a similar behavior of MgO even in these complex slags. Figure 9 shows the effect of MgO content on the reduction rate of Cr_2O_3. The reduction rate has a minimum at 5% MgO at all temperatures.

3.3. Effect of Basicity

The effect of basicity (wt%CaO/wt%SiO_2) of the slag on the reduction rate of Cr_2O_3 was not very significant. However, the rate constants for slags of 1.0 basicity were found to be larger than those of 1.5 basicity at all the three temperatures studied. This observation is in confirmity with a recent study on the Cr_2O_3 reduction[11]. They reported the effect of basicity on the rate of Cr_2O_3 reduction in the range 0.8 to 2.0. It may be mentioned that a slag of basicity 1.8 was also investigated but it did not melt at any of the experimental temperatures. This suggests that the melting point of the slag was more than 1923 K.

3.4. Effect of V_2O_5 Content

Figure 10 shows the effect of V_2O_5 on the reduction rate of Cr_2O_3 with temperature. The rate constant decreased with increase in V_2O_5 content in the slag. This may be due to the competition between Cr_2O_3 and V_2O_5 for reduction on fixed available sites (iron droplets saturated with carbon).

3.5. Activation Energy

Figure 11 represents the ln (α) vs. 1/T plot for various slag compositions. The activation energies for the reduction in slags represented by the initial wt% Cr_2O_3 of 2, 10 and 14 were 101, 342 and 531 kJ/mol respectively. Activation energy of 201 kJ/mol in a slag containing 5% Cr_2O_3 was reported in a previous work[13]. The variation of activation energy for Cr_2O_3 reduction with % Cr_2O_3 for all the slags studied along with the value obtained in the previous work[13] is plotted in Fig. 12. Literature data[14-17] available on the activation energy for Cr_2O_3 reduction ranges from 93 kJ/mol to 316 kJ/mol. It can be seen from the plot that the activation energy values range from 100 kJ/mol to 530 kJ/mol in the present study.

The reported values for the diffusion of oxygen ions in slags are 355[18] and 397[19] kJ/mol. The mechanism for Cr_2O_3 reduction in slags having the activation energy values in the range 300-400 kJ/mol in the Fig. 12 can therefore be considered to be the oxygen ions diffusion in slag phase. The mechanism in slags having the activation energies in the range of 100 kJ/mol could be the diffusion of chromium in metal phase since the reported values for chromium diffusion in Fe-C alloys are 69[20] and 66.9[21] kJ/mol. The mechanism is mixed controlled in slags having intermediate values of activation energies.

Figure 13 shows the variation of activation energy with average gas generation rate in the steady state region of Cr_2O_3 reduction at 1823 K. The graph shows that slags having gas generation rate less than 0.08 lt./min had activation energies of about 300 kJ/mol and above. The slags having gas generation rate greater than 0.11 lt./min had activation energies less than 170 kJ/mol. The mixing of the slag melt during the progress of the reaction depends on the rate of gas evolution. If the mixing is intense, the length of diffusion path in the slag is low and the rate controlling step becomes diffusion in the metal phase. If the stirring intensity is less, then the reduction becomes slag phase diffusion controlled. It can be seen from the figure that V_2O_5 content in the slag had practically no effect on the mechanism of the reduction.

4. Discussion

Heterogeneous reactions take place at the interface between the reactants and the rates depend on the available contact area. The reduction of Cr_2O_3 in the slag takes place both at the graphite/slag and metal/slag interface. In the present case, the contact area available for reduction is not well defined. Since the iron droplets present in the slag act as sites for reduction of Cr_2O_3, the rate of reduction changes with the number of droplets present and their size in the slag at any instance. In few cases small liquid droplets were observed in the foam indicating that some of the slags had much larger surface area for reduction.

Figure 1 shows that the reduction does not take place uniformly at the bottom of the graphite crucible. The contact area for reduction by graphite depends on the extent of slag foaming. It becomes insignificant if there is severe foaming. The foam characteristics change with slag

properties such as viscosity and surface tension, which are dependent on the slag chemistry. The foam height also varied with time for a given slag composition. Therefore, the contact area for both metal/slag and graphite/slag interfaces varied with the experimental conditions.

In the slag containing 5% MgO liquid droplets were present at the bottom of the crucible and their size reduced with the progress of the reaction. However, in the slag containing very low MgO content small liquid droplets were found suspended in the foam suggesting that the surface area for Cr_2O_3 reduction was much larger in this slag than in the former. So, the higher reduction rates in Fig. 9 for slag containing very low MgO content may be attributed to the change in the available surface area for reduction. It was observed that in the slags containing V_2O_5, severe foaming took place and in some cases most of the slag melt was lifted upwards for long periods thereby reducing contact of the slag with the bottom of the crucible. The reduction in rates for slags containing increasing amounts of V_2O_5 shown in Fig. 10 may be due to decrease in the contact area.

In order to indicate the uncertainty of contact area for reduction process, the variation of rate constant, α, with temperature was plotted in Fig. 14 for the slag containing 5% Cr_2O_3. This plot shows that temperature had practically no effect on the rate constant for Cr_2O_3 reduction. This may be due to the decrease in the surface area available for the reduction at higher temperatures.

The calculation of activation energies has been carried out with the assumption that the surface area available for reduction of Cr_2O_3 is constant for a slag and is independent of temperature. Although the above discussion points out the uncertainty in the surface area of reaction, the trend shown in Fig. 13 indicates that, in general, the assumption is valid.

5. Conclusions

Several phenomena such as non-uniform gas evolution, foam and emulsion formation and dissolution of Al_2O_3 took place during the simultaneous reduction process. There was no direct relationship between the gas generation rate and foam height. The surface area of reduction is not clearly defined and is not same for all slags.

The reduction rate of Cr_2O_3 is not affected by the Al_2O_3 content of slag and the influence of basicity is not very significant. The rate has a minimum at 5% MgO. An increase in V_2O_5 content of the slag decreases the reduction rate. The effect of MgO and V_2O_5 on the rate is primarily due to the change in surface area for reduction.

The activation energies for the reduction of Cr_2O_3 range from 100 kJ/mol to 530 kJ/mol. The mechanism for the reduction of Cr_2O_3 depends on the intensity of stirring due to the in-situ gas generation. At high and low gas generation rates the reduction is controlled by diffusion in the metal and slag phases respectively.

References

1. H. G. Katayama, M. Satoh, M. Tokuda: "Fundamental Study on Smelting Reduction of Chromite Ore powder", *Conf. Proc. of 7th Proc. Tech. Conf.*, Vol. 7, Toronto, Canada, (1988), pp. 125-129.

2. S. Fukagawa, T. Shimoda: "Smelting Reduction Mechanism of Chromite Ore Sinter by Solid Carbon", *Trans. ISIJ*, Vol. **27**, No. 8, (1987), pp. 609-617.

3. S. Yokoyama, M. Takeda, K. Ito and M. Kawakami: "Rate of Smelting Reduction of Chromite Ore by Dissolved Carbon in Molten Iron and Slag Foaming during the Reduction", *Tetsu-to-Hagané*, Vol. **78**, No. 2, (1992), pp. 29-36.

4. W. Pei and O. Wijk: "Mechanism of Reduction of Chromium Oxide Dissolved in CaO-SiO_2-MgO-Al_2O_3 Slag by Solid Carbon", *Scand. J. of Met.*, Vol. **22**, (1993), pp. 30-37.

5. F. Fun: "Rates and Mechanisms of FeO Reduction from Slags", *Metall. Trans.*, Vol. **1**, (1970), pp. 2537-2541.

6. Y. Zhou, T. Du: "Reaction Rate of Smelting Reduction", *Proc. of Shenyang Int. Symp. on Smelting Reduction*, Sept. 3-5, (1988), pp. 147-159.

7. G. Graenzdoerffer, W. M. Kim and A. H. Fine: "Kinetics of the Reduction of FeO_x from Molten Slag", *Proc. of the Process. Tech. Conf.*, Vol. **7**, Toronto, Canada, (1988), pp. 137-143.

8. B. Sarma, A. W. Cramb and R. J. Fruehan: "Reduction of FeO in Smelting Slags by Solid Carbon: Experimental Results", *Metall. Mater. Trans.*, Vol. **27B**, No. 5, (1996), pp. 717-730.

9. K. Ito and R. J. Fruehan: "Study on the Foaming of $CaO-SiO_2$-FeO Slags: Part I. Foaming Parameters and Experimental Results ", *Metall. Mater. Trans.*, Vol. **20B,** No. 4, (1989), pp. 509-514.

10. M. Maeda and N. Sano: "Thermodynamics and Kinetics of the Reduction of Chromium Oxide in Silicate Melts", *Conf. Proc. of 6th Proc. Tech. Conf.*, Vol. **8**, Washington D.C., U.S.A, pp. 735-740, 1986.

11. M. Görnerup and A. K. Lahiri: "Study of the Reduction of EAF Slags in Stainless Steelmaking. Part I: Observations", *Ironmaking and Steelmaking*, Vol. **25**, (1998), pp.317-322.

12. J. H. Swisher and C. L. McCabe: "Cr_2O_3 as a Foaming Agent in $CaO-SiO_2$ Slags", *TMS-AIME,* Vol. **230,** No. 12, (1964), pp. 1669-1675.

13. M. Görnerup and A. K. Lahiri: "Study of the Reduction of EAF Slags in Stainless Steelmaking. Part II: Mechanism of CrO_x Reduction", *Ironmaking and Steelmaking*, Vol. **25**, (1998), pp. 382-386.

14. C. N. Anyakwo: "The Kinetics of Cr_2O_3 Reduction from Slags by Carbon Dissolved in Molten Iron", *Diss. Abst. Int.*, Vol. **49**, No. 10, (1989), p.295.

15. O. Demir and R. H. Eric: "Reduction of Chromite in Liquid Fe-Cr-C-Si Alloys", *Metall. Trans.*, Vol. **25B**, No. 4, (1994), pp. 549-559.

16. L. Zhang, Z. Zou, A. Liu and Z. Xiao: “Kinetics of Chromite Smelting Reduction", *J. Northeastern University*, Natural Science (Shenyang, China), Vol. **17**, No. 3, (1996), pp. 252-255.

17. T. Shimoo, T. Isobe, S. Ando and H. Kimura: “Mechanism of Reduction of Chromium Oxide in Alumina Slag by Solid Carbon", *J. Jpn. Inst. Met.*, Vol. **50**, No. 7, (1986), pp. 646-653.

18. F. Oeters: “Convective Diffusion with Chemical Reaction", *Conf. Proc. of Kinetics in Metallurgical Processes in Steelmaking*, Aachen, Germany, (1975), p. 116.

19. G. H. Geiger and D. R. Poirier: “Transport Phenomena in Metallurgy", Addison-Wesley Publ. Co., Reading, Massachusetts, U.S.A. (1973), p. 462.

20. Y. Ono, T. Yagi: “Diffusion of Cr, Mn, Co and Ni in molten iron saturated with carbon", *Trans. ISIJ*, Vol. **11**, No. 4, (1971), pp. 275-279.

21. “Handbook of Physico-chemical Properties at High Temperatures", Y. Kawai and Y. Shiraishi (Editors), The Iron and Steel Institute of Japan, Special Issue No. 41, (1988), Tokyo, Japan.

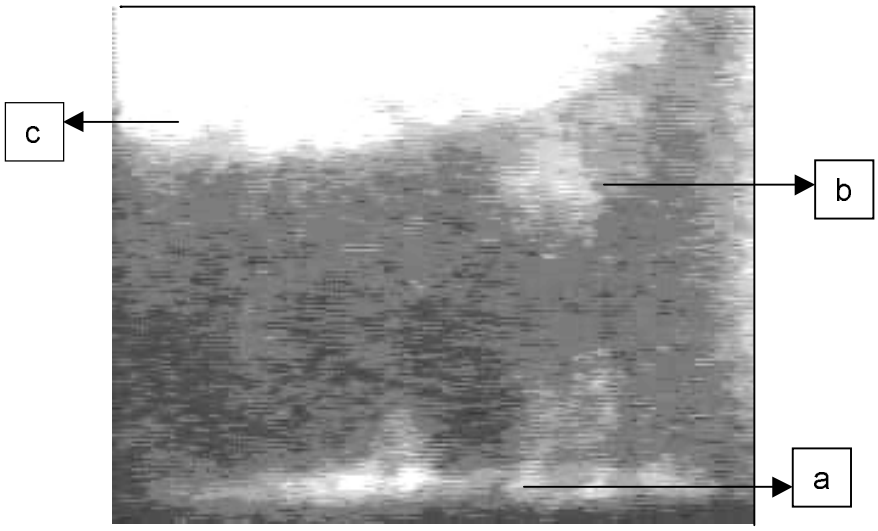

Fig. 1. X-ray image showing the reduction process of the slag in a graphite crucible. (a) Gas generation, (b) Bubble coalescence and (c) Bubble collapse and splashing.

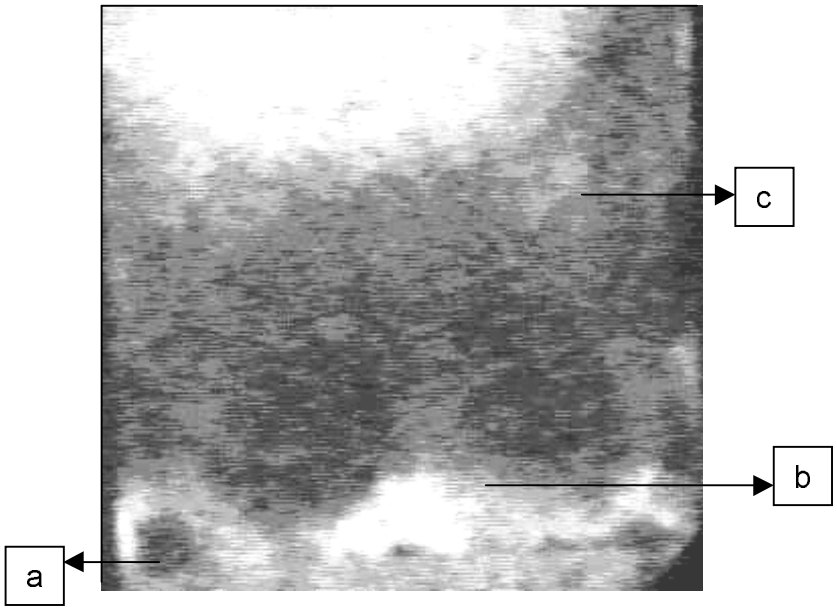

Fig. 2. X-ray image showing several distinct features. (a) Iron droplet, (b) Gas evolution and (c) Bubble coalescence.

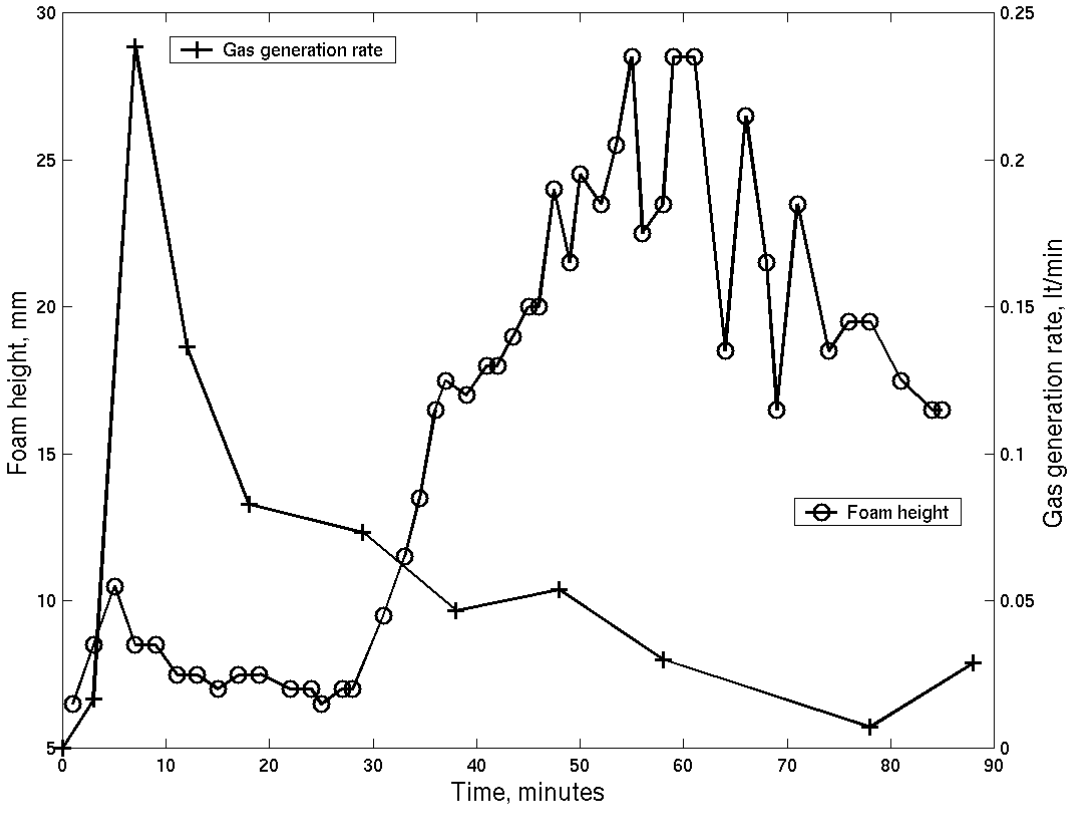

Fig. 3. The variation of foam height and gas generation rate with time for a slag of composition 5%MgO, 7% Al_2O_3, 2% MnO, 6% FeO and 10% Cr_2O_3 at 1823 K.

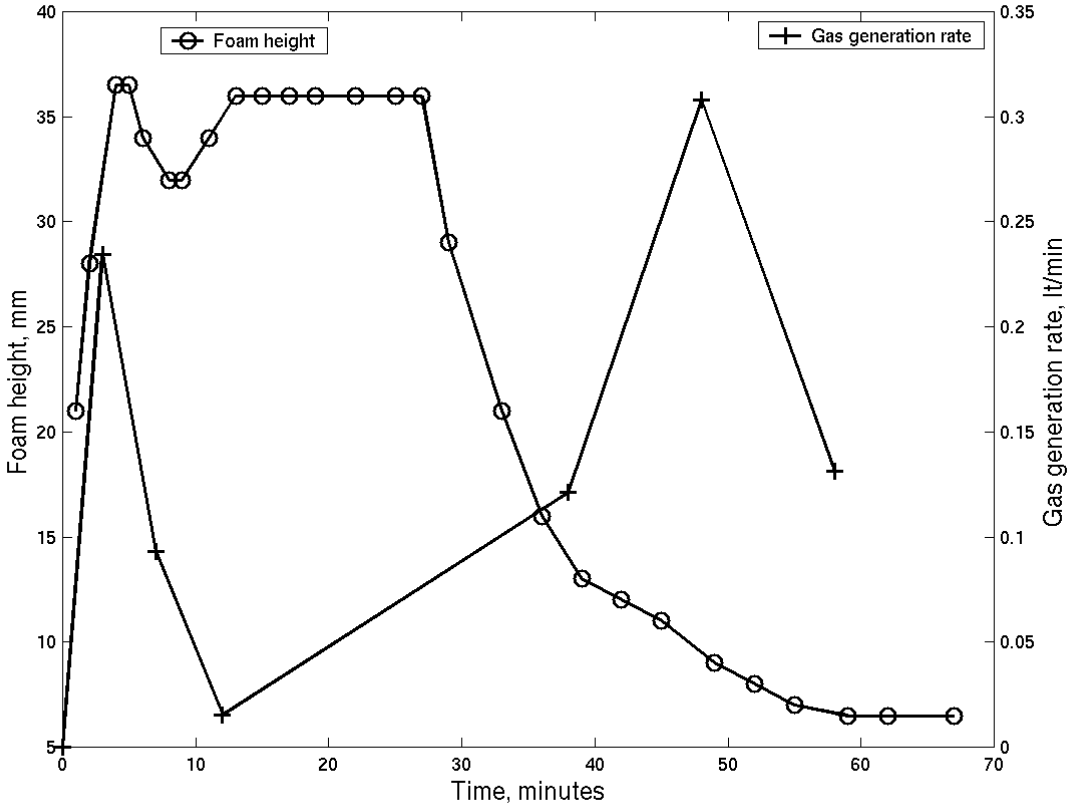

Fig. 4. The variation of foam height and gas generation rate with time for a slag of composition 5% MgO, 7% Al_2O_3, 2% MnO, 6% FeO, 5% Cr_2O_3 and 5% V_2O_5 at 1923 K.

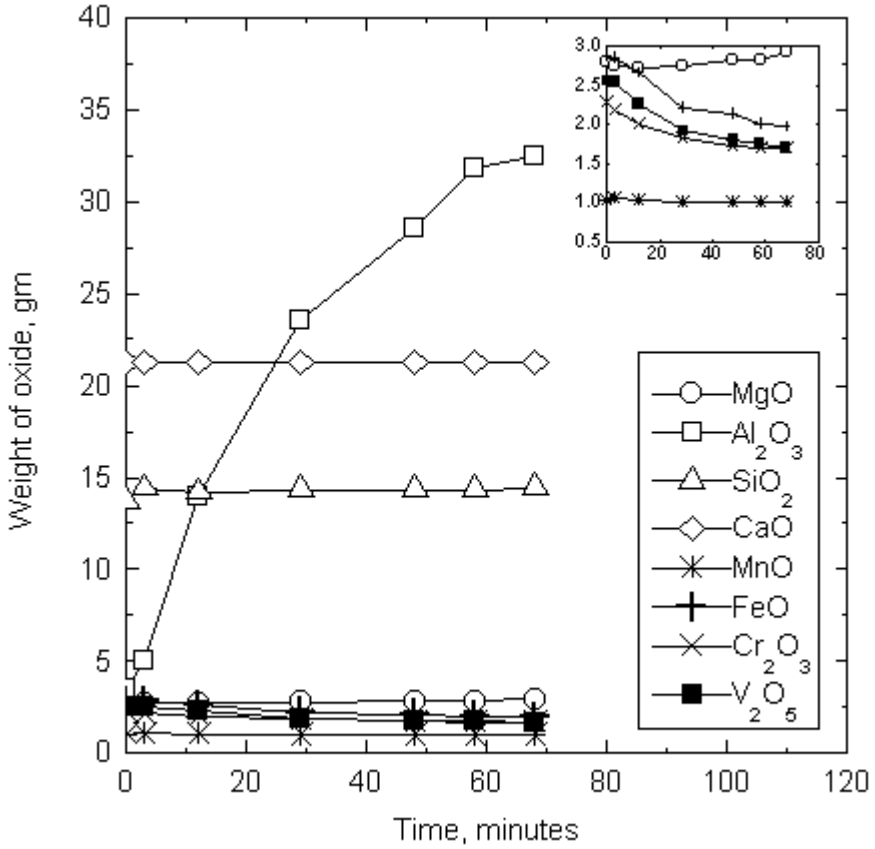

Fig. 5. Experimental results for a slag containing 5% MgO, 7% Al_2O_3, 2% MnO, 6% FeO, 5% Cr_2O_3 and 5% V_2O_5 at 1823 K.

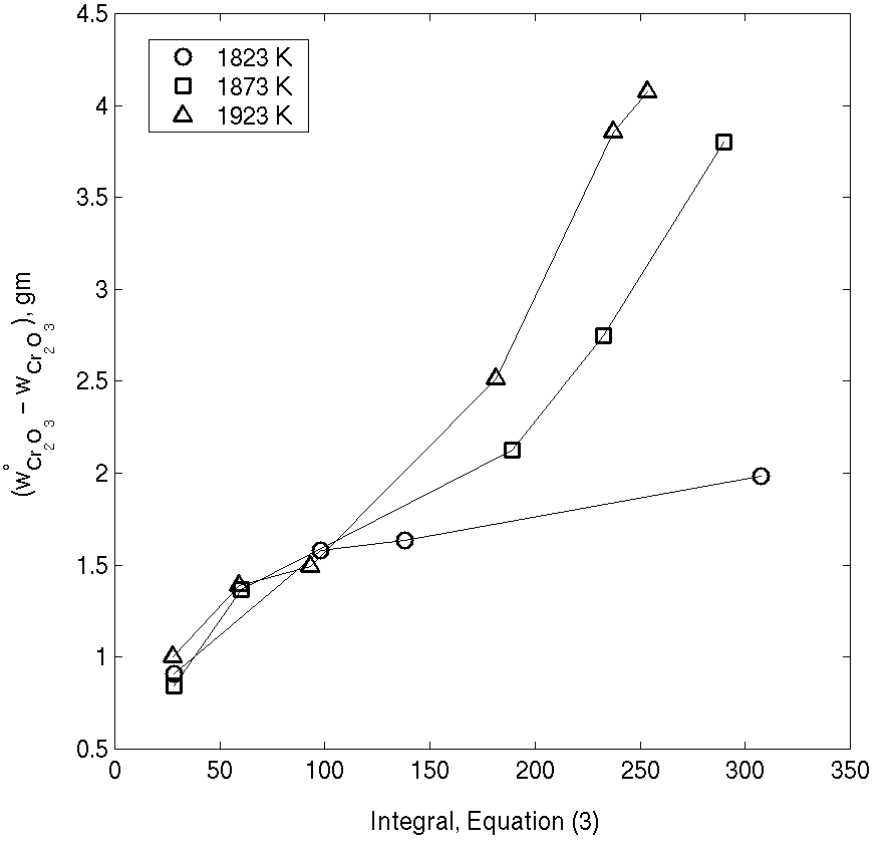

Fig. 6. Reaction process for a slag containing 5% MgO, 7% Al_2O_3, 2% MnO, 6% FeO and 10% Cr_2O_3 at 1823 K.

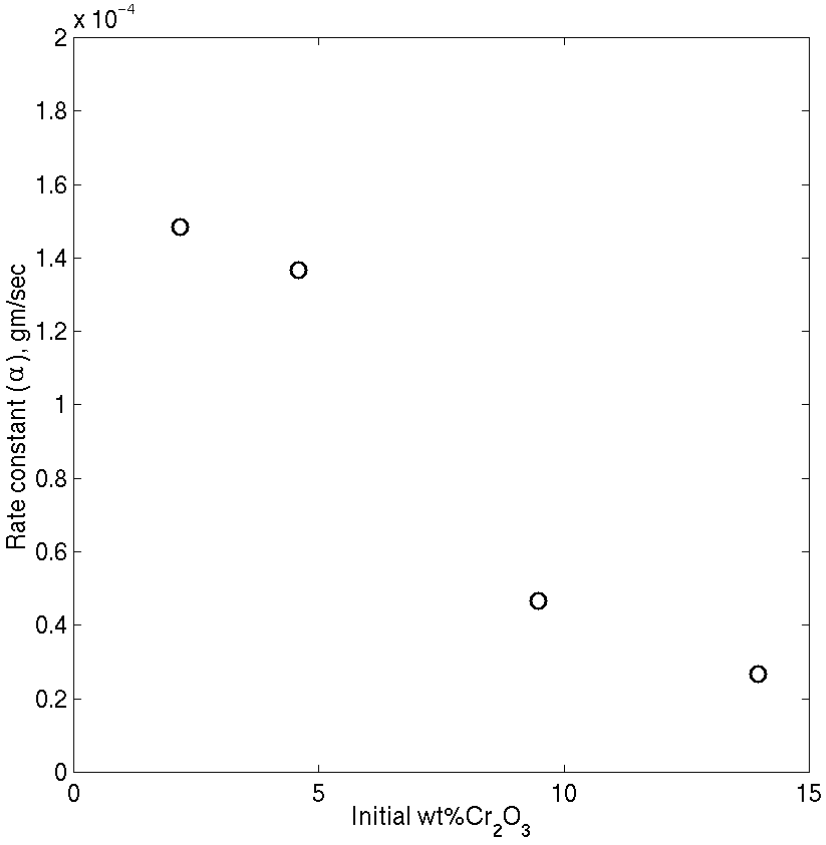

Fig. 7. The effect of initial Cr_2O_3 content in the slag on the rate of Cr_2O_3 reduction.

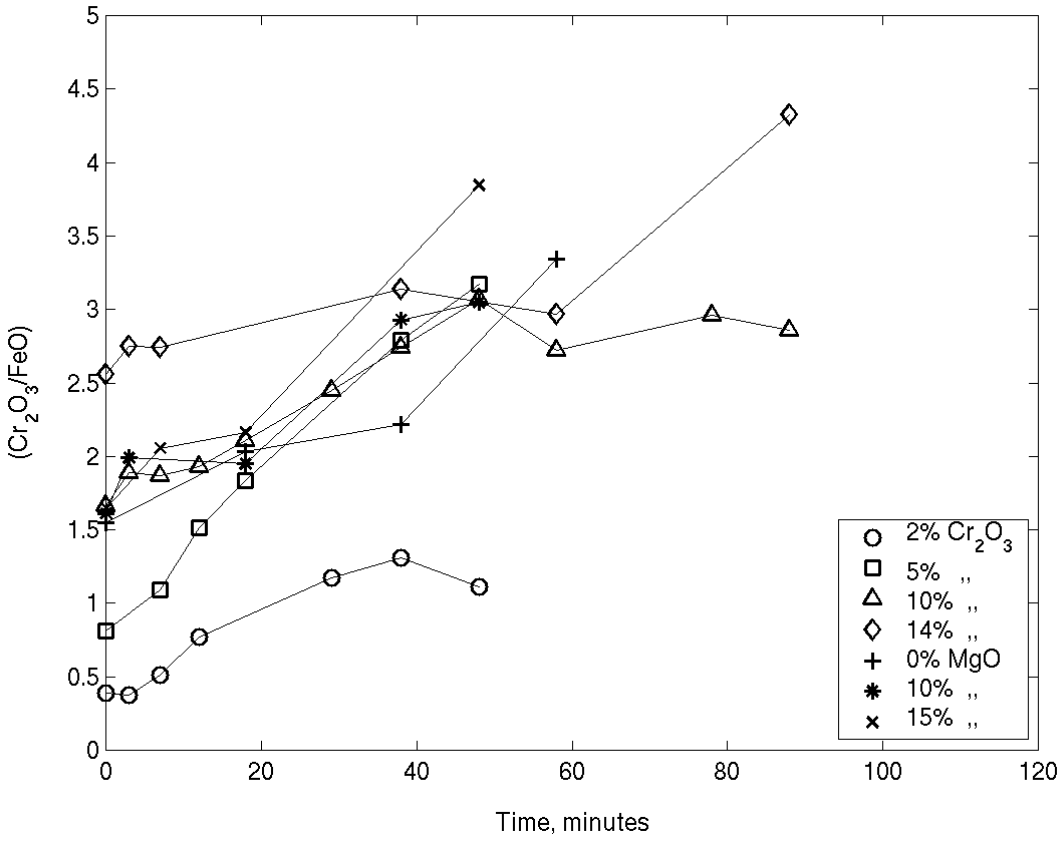

Fig. 8. The variation of Cr_2O_3/FeO ratio with time for various slags at 1823 K. The symbols refer to various amounts of Cr_2O_3 and MgO in the typical slag composition given in Table I.

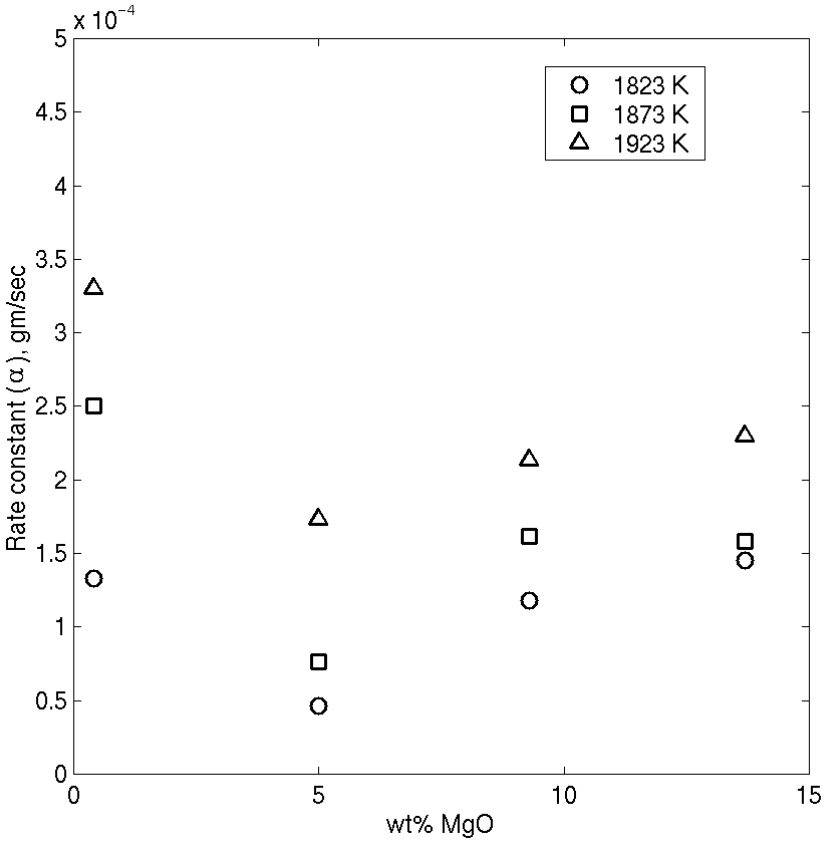

Fig. 9. The effect of MgO content in the slag on the reduction rate of Cr_2O_3.

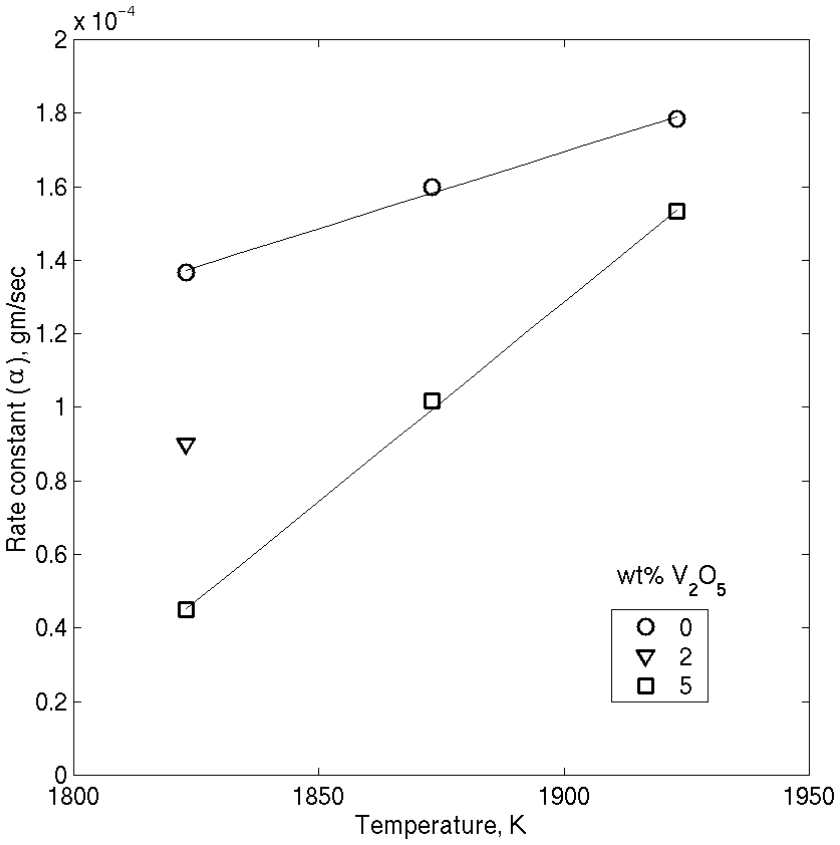

Fig. 10. The effect of V_2O_5 content in the slag on the reduction rate of Cr_2O_3 with temperature.

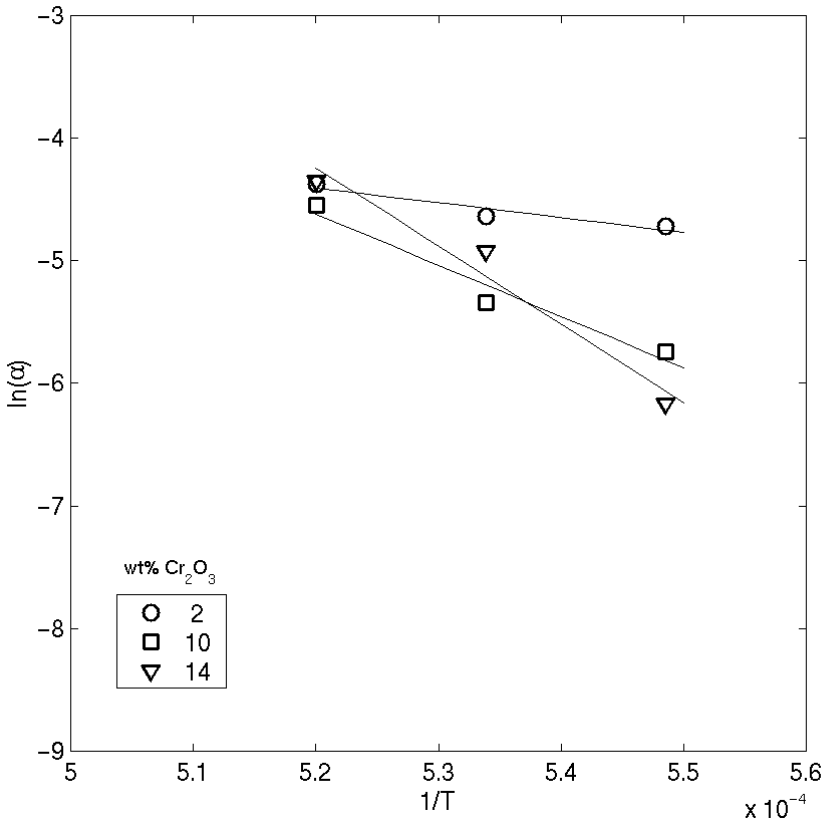

Fig. 11. The plot of ln (α) versus 1/T of Cr_2O_3 reduction for slags containing various amounts of Cr_2O_3.

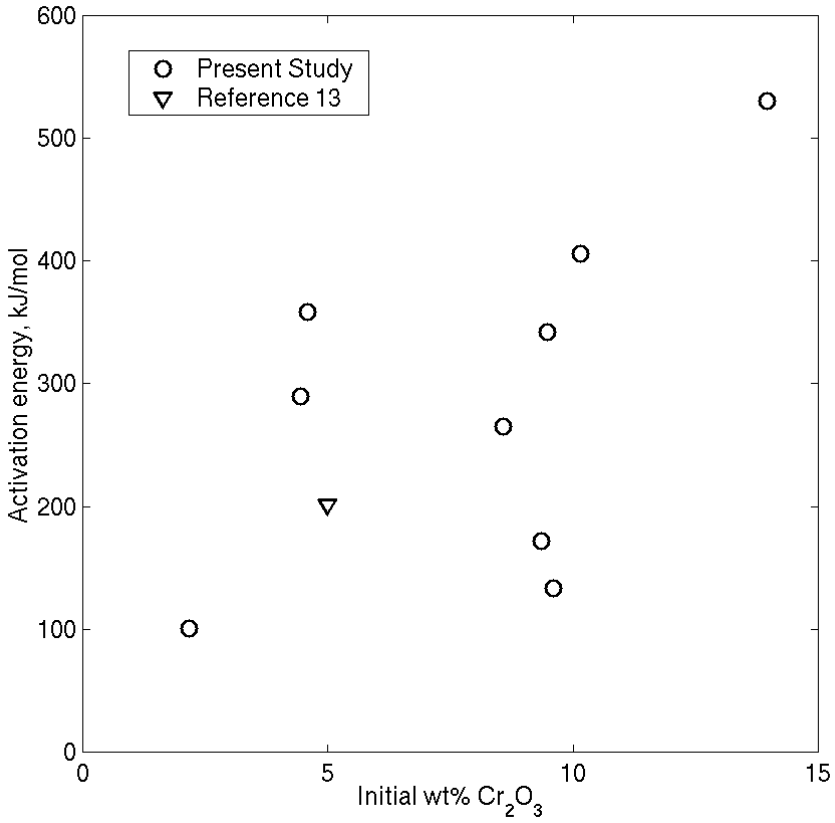

Fig. 12. The effect of initial Cr_2O_3 content on the activation energy for Cr_2O_3 reduction in different slags.

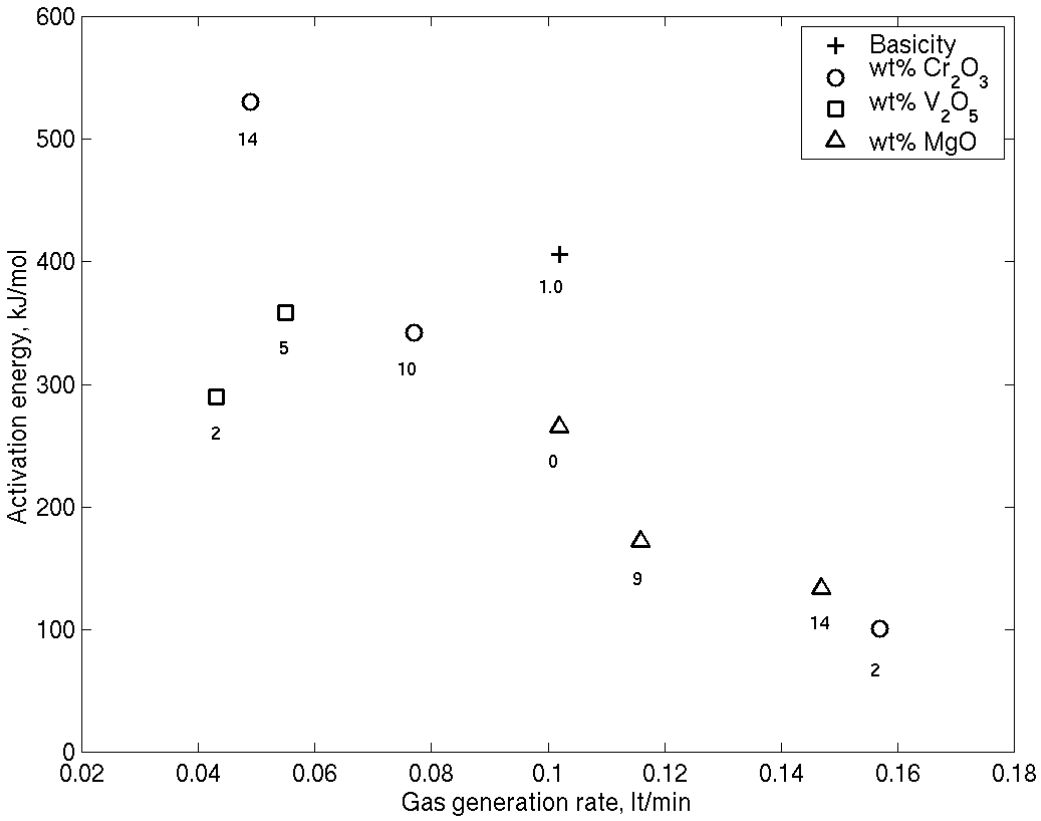

Fig. 13. The effect of gas generation rate on the activation energy for Cr_2O_3 reduction for various slags at 1823 K. The base slag composition is 7% Al_2O_3, 6% FeO, 5% MgO, 10% Cr_2O_3 and 2% MnO, Basicity = 1.5.

+: Basicity = 1.0; Δ: base slag with varying wt% MgO; O: base slag with varying Cr_2O_3 content; □: base slag with varying V_2O_5 content.

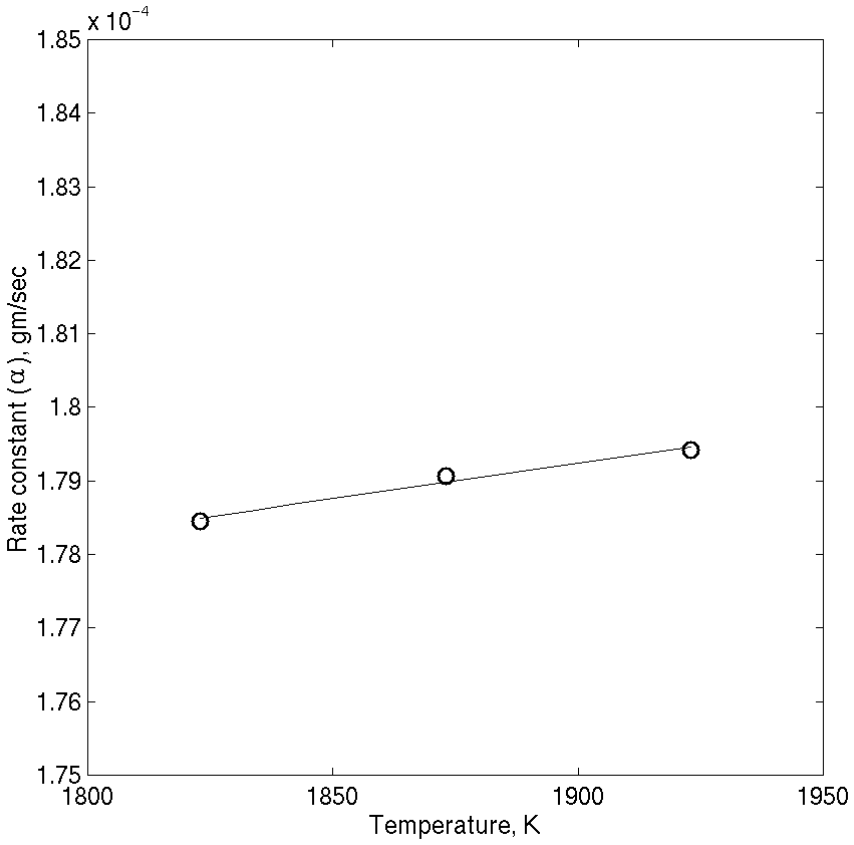

Fig. 14. The variation of rate constant with temperature for the slag containing 5% MgO, 7% Al_2O_3, 2% MnO, 6% FeO and 5% Cr_2O_3.

Table I

Typical Slag Composition

Basicity = wt%CaO / wt%SiO_2

Basicity	wt% Al_2O_3	wt% FeO	wt% MgO	wt % Cr_2O_3	wt% MnO
1.5	7	6	5	10	2

Table II

Slag Compositions Studied

Basicity = wt%CaO / wt%SiO_2

Basicity	wt% Al_2O_3	wt% FeO	wt% MgO	wt% Cr_2O_3	wt% MnO	wt% V_2O_5
1.0, 1.5	4, 7	0, 6, 10	0, 5, 10,15	2, 5, 10, 14, 20	0, 2, 4	0, 2, 5